Flood Area Estimation using Personal Location Data - Case Study of Japan Floods in 2018 -

Kei Hiroi
Graduate School of Engineering
Nagoya University
Nagoya, Japan
k.hiroi@ucl.nuee.nagoya-u.ac.jp

Takahiro Yoshida
Center for Global Environmental Research
National Institute for Environmental Studies
Tsukuba, Japan

Yoshiki Yamagata
Center for Global Environmental Research
National Institute for Environmental Studies
Tsukuba, Japan

Nobuo Kawaguchi
Graduate School of Engineering
Nagoya University
Nagoya, Japan

***Abstract*—This research proposes a flood area estimation method in urban areas using personal location data. Many studies have investigated the estimation of flood levels; however, the majority of these previous works are based on the flood monitoring data. The main cause of flood disaster death is drowning due to evacuation delay in the area where observation equipment is not installed, so it is difficult to estimate flood occurrence by the previous method based only on monitoring data. In this research, we propose an estimation method that does not rely on monitoring data and instead estimates flood areas using GPS data collected from smartphones owned by the affected people. This method detects anomaly areas to analyze temporal and spatial changes of an area where a personal movement during a flooding event differs from that during regular times from personal location data. For anomaly detection, we use a dynamic time warping method with fixed window size and inequality metrics to estimate the area where an anomaly event occurred in 2 km grids. We applied this method to Kurashiki city, Okayama Prefecture, where there 52 people died during a flood that occurred in Japan in 2018. Our method found that, at the flooding time, the anomaly occurrence was estimated correctly in the area where inundation actually occurred.**

***Index Terms*—Disaster Estimation, Anomaly Detection, GPS Data**

I. Introduction

There are concerns that the risk of floods on the global scale will intensify. The IPCC's Fifth Assessment Report stated that global warming is gradually progressing, and it is likely that the frequency and intensity of rainfall will change accordingly [1]. There are already many areas where the frequency and intensity of heavy rain and flooding are increasing worldwide [7] [9]. As one type of flooding countermeasure, risk analysis studies aim to utilize the land vulnerability analysis for flood control through urban construction and town development against disasters [10] [13] [6]. For large rivers, the development of prediction technology based on water level observation data has been researched to precisely detect floods in advance. Some observation methods using wireless sensor network (WSN) studies feature smaller equipment for water monitoring sensors [7], multiple sensing [8], WSNs for alerts [9], and resilient data communication networks [10]. Approaching flood prediction, hydrological techniques [11] or artificial neural networks [12] [13] based on the flood level data are proposed as good prediction methods.

However, before flooding of a large river occurs due to a large amount of rain, water overflowing onto the adjacent road may occur and make evacuation difficult. This is a phenomenon called inundation flooding. The water level monitoring of the road is necessary to detect flood occurrence; nevertheless, road monitoring for flooding has hardly been carried out. In addition, almost no road flooding has been observed, since the damage caused by inundation flooding is smaller than that of flooding of a large river. Inundation flooding may cause inundation of several tens of centimeters to several meters.

Recent flood disaster surveys have pointed out that the occurrence of inundation flooding may cause the damage of river floods to be greater. Inundation flooding has already occurred by the time a large river flood is detected; therefore, there is a high possibility that the affected people cannot evacuate to shelters. The victims who cannot evacuate will suffer the damage from a large river flood that occurs after inundation flooding. In Japan, the heavy rain in Kita-Kyushu in 2017 (18 people dead due to flooding) and heavy rain in western Japan in 2018 (over 200 people dead) caused many deaths because inundation flooding prevented evacuation to escape the flood waters. For this reason, we believe that it is necessary to detect the occurrence of inundation floods, even for areas where water level observation equipment is not installed.

This paper proposes a spatial-temporal anomaly estimation method using personal location data. By applying this method

978-1-5386-9151-9/19/$31.00 ©2019 IEEE

to areas that have a high possibility of flood occurrence, we detect anomaly events such as flooding even in areas where observation equipment is not installed. This anomaly estimation method calculates the characteristics of personal location data; moreover, the method investigates the spatial and temporal changes of the characteristics. Spatial-temporal anomaly estimation is performed by extracting the time and area in which the change deviates from those of regular time. We apply this method to Mabi town, Kurashiki city, Okayama Prefecture, where 52 deaths occurred because of heavy rain in 2018. In addition, we consider a method for estimating road conditions of the area detected as an anomaly area. In Japan, large flood often occurs in areas with low population. Thus, it was difficult to determine the tendency of people's movement using previous GPS data analysis methods in flood disaster situations. This paper is an anomaly detection method that can be applied even in areas with small personal location data.

II. Related Work

There are several papers that report detecting urban anomaly states based on human behavior. Sakaki proposed an algorithm to monitor tweets and to detect earthquake events [14]. He considered each Twitter user as a sensor and applied Kalman filtering and particle filtering, which are widely used for location estimation in ubiquitous/pervasive computing. Weng tried to detect flood events by analyzing the text stream in Twitter with clustering of wavelet-based signals [15]. Seonhwa developed a real-time monitoring system of social big data to monitor disaster situations and trends in real time and draw conclusions from big tweet data [16]. The system crawls social big data, especially Twitter, analyzes the disaster-related tweets in real time, and displays disaster issues and trends on a map.

In recent years, to determine the population distribution in disaster areas, resource utilization for rescue, and optimal placement of human resources, many studies have analyzed and predicted the movement of people and vehicles during disasters using GPS data obtained from mobile phone base stations and their statistical distributions. Witayangkurn reported a system for detecting anomalous events, such as earthquakes, in grid-based areas using large-scale GPS data [17]. Their system used a hidden Markov model to construct a pattern of the spatial-temporal movements of people in each grid during each time period. Madey developed an application using real-time cell phone calling data from a geographical region, including calling activity [18]. The application tried to analyze the movement and calling patterns of the population using the cell phones in a geographical region to serve as ad hoc mobile sensor networking. This application is used for various aspects such as a service that identifies passable roads from the movement of cars and a prediction method that simulates the movement of people in a wide area immediately after the occurrence of an earthquake. Gerla presented a system for detecting traffic congestion and incidents from real-time GPS data collected from GPS trackers or driver smartphones [19]. The simulated results on incidents showed a detection rate of 91.6%. However, GPS data at the time of a flood disaster do not have as wide an area as that during an earthquake disaster. It is considered that the absolute number of data is small depending on the region. Consequently, it is an issue that the tendency of people movement during flooding is difficult to determine.

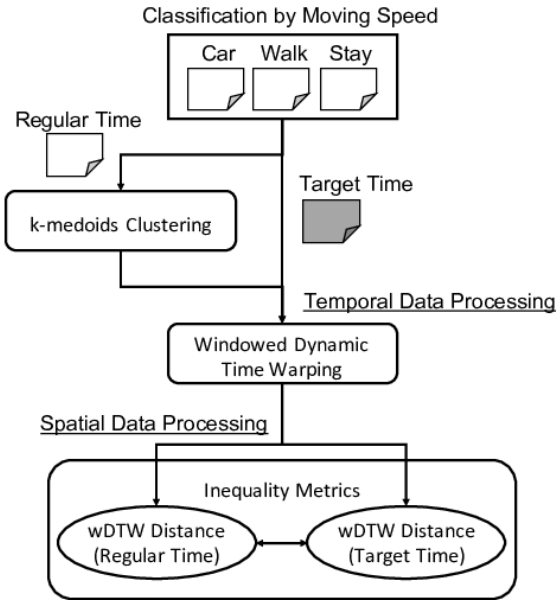

Fig. 1. Proposed Estimation Method

III. Flood Estimation Method

A. Overview

Processing of the proposed method is shown in Figure 1. In this method, we estimate the flooded area by extracting temporal and spatial changes to divide the area into detailed grids, which is a difficult task even with a small number of location data. This method consists of two processes, temporal data processing and spatial data processing. First, we divide the target area into 2-km grids. As temporal data processing, we classify the location data of each grid with clustering using the k-medoids method. Then, we calculate the time series data expressing the difference from the regular time to compare the characteristics of clustered data to personal location data at a target time. For this characteristic comparison, we improve the dynamic time warping (DTW) method as windowed dynamic time warping (wDTW), which is a method for quantifying the similarity between several time series data. For spatial data processing, we detect the anomaly area to compare the characteristics of each grid using inequality metrics with the time series data calculated by the temporal data processing.

B. Classification by Moving Speed

First, we calculate the moving speed from the location data recorded on the server and classified by speed using a method of [20]. The moving speed is calculated from the difference of the previous time/location of the unique ID. Then, we classify

the data into three groups of 0.0-0.5 km, 0.5-5.0 km, over 5.0 km according to the moving speed. The ID of 0.0-0.5 km speed is "stay state", the ID of 0.5-5.0 km speed is "walk", and the ID of more than 5.0 km speed is equivalent to the movement by "car". Here, the data with recorded intervals exceeding 30 minutes are excluded because it is difficult to accurately determine the moving speed during this timeframe. It may be considered that multiple movements are included within 30 minutes. Since the classification in this paper is not a distinction of a means of transportation, but a method to classify how far the affected people moves in a certain time, we use a simple classification method based on distance and time. Through this processing, we calculate time series data consisting of unique ID, latitude/longitude, and moving speed.

Furthermore, the target area (here, the area that has a high possibility of flood occurrence) is divided into n grids of k km. For n grids, the total number of unique personal location data existing in the corresponding grid is calculated every 15 minutes for the time series data. Although the smaller the value of k, the more the detected area becomes detailed, if k is too small, the total number of unique personal location data existing in the grid decreases, and detection becomes difficult.

C. Clustering

We perform clustering on the time series data of n obtained for location data during a regular time. The DTW distance is calculated for n time series data using DTW. DTW calculates the DTW distance by $D_{i,j}$ of all combinations for similarity matrix D of $M \times N$ with the following equation.

$$D_{j,j} = \sqrt{(x_i - y_j)^2} + min(D_{i,j-1}, D_{i-1,j}, D_{i-1,j-1}) \quad (1)$$

The DTW distance of x_t and y at the time of $t \times 15$ minutes is $D_{t,N-1}$. Each M, N is the length of time series data x,y. For the obtained n number of distance matrices $D_{M-1,N-1}$, we process clustering of the time series data using the k-medoids method, which is based on similarity. This paper uses personal location data collected only from the smartphone on which the application is installed. It is considered that this data has statistical sampling bias. Therefore, we did not use clustering methods like Mean-Shift Clustering or Density-Based Spatial Clustering of Applications with Noise based on spatial density. The k-medoids method is to select k medoids from N data sets. Then, the method finds the nearest neighbor medoid among k medoids for $N - k$ pieces of data and allocates data to the cluster to which the medoid belongs (L is the cluster number). The medoid of the cluster is updated based on

$$\arg\min_{i \in C_i} \sum_{j=1}^{n_l} d(x_i, x_j) \quad (2)$$

By the processing, the time series change of the total number of unique location data of each grid at the regular time is classified into l number of clusters. Then, we obtain l number of clustered time series data to calculate the average value of the total number of unique location data for each cluster every time t using regular time data.

D. Windowed Dynamic Time Warping

Regarding the location data of each grid at the time of flood occurrence, we calculate the difference in time series change from the regular time. For each grid on the target date, we compare clustered time series data of the same day before the month calculated by k-medoids clustering as the regular time. The difference between the time series change of the regular time and the target date is calculated using the expression (1). Here, for DTW, the window width of the distance matrix calculation is divided into constant widths; we call it wDTW. For x_i of target data, we determine the window width of y as $j = t-2\ t+2$ to compare the time series data y_j. To calculate the distance matrix, data processing is performed to determine whether a large difference occurs within 30 minutes before and after the time t. We perform this processing for each t, to calculate time series data of the wDTW distance between the regular time and the target date for each grid.

E. Inequality Metrics

Here, by calculating inequality metrics, the area in which the anomaly event has occurred is estimated in the target area. For calculating inequality metrics, we use the Gini coefficient (Equation (3)), which is a measure of the degree of inequality between regions. The number of each grid is $i = (1, 2, ..., n)$, and the region attribute z_i is the wDTW distance. We define the wDTW distance of the target grid as z_j. $\overline{z}$ represents the sample mean of wDTW for all grids.

$$G = \sum_{i=1}^{n} \sum_{j=1}^{n} \frac{|z_i - z_j|}{2n^2} \overline{z} \quad (3)$$

The Gini coefficient shows that the closer the value is to 1, the greater the regional inequality. When the Gini coefficient is large, we estimate the large grid of spatial Gini coefficient $G_{i,j}$ as the area of anomaly occurrence. In this study, the area where this anomaly occurs is calculated based on the moving speed. We focus on the possibility that actions that can be carried out in other areas cannot be performed in the target area if the moving speed is particularly different in that area. Specifically, the moving speed of a car in other grids is based on evacuation orders; in other words, although the car is evacuating, if movement is not observed in a certain grid, we consider the possibility that the car cannot move due to an influence such as flooding.

IV. Analysis of Actual Flood Case

A. Flooding Case of Japan Floods in 2018

In this evaluation, to detect the flooded area, we use personal location data for a flood disaster that occurred in western Japan in 2018. This flood disaster occurred due to torrential rains caused by Typhoon No. 7 and a seasonal rain front from June 28 to July 8, 2018. In Kurashiki city, Okayama Prefecture, Japan, a sediment-related disaster alert was announced on July

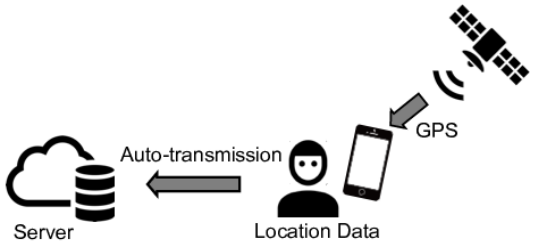

Fig. 2. Personal Location Data using GPS Data

5, and a heavy rain special alert was issued at 19:40 on July 6. Due to the continuing rain, an evacuation advisory was issued at Mabi town in Kurashiki city through 22:00 on July 6. At 22:20, the Oda River reached the flooding danger level. The area on the right bank of the Oda River was under a mandatory evacuation order at 23:45. Additionally, flooding occurred in the Oda River at 0:30 on July 7. A mandatory evacuation order was issued to the area on the left bank of the Oda River at 1:30.

Mabi town in Kurashiki city was widely flooded by morning since the embankments of the Oda River and the tributary to the Oda River were broken down. Flooding occurred in the Oda River at 0:30 July 7, and an evacuation order was announced at 1:30 on the left bank of the Oda River. 51 people died in Mabi town. Most victims appear to have died by drowning. Of the victims, 43 were were found indoors, and 42 of them were found on the first floor of their homes. According to a survey by the Japan Society of Civil Engineers, the depth of flooding exceeded 5 meters. Moreover, the level appeared to reach a maximum of 5.4 meters. The floods covered 1,200 ha, which is one-quarter of Mabi town.

B. Personal Location Data

This research uses GPS data obtained from smartphones as anonymized personal location data (the data were provided from Blogwatcher[1]). Specific applications collect latitude and longitude location data (Figure 2). The smartphone location data are automatically transmitted to the server every 15 minutes.

The location data consist of detection time, latitude, longitude and unique uuid. We use the location data of Mabi town from 18:00 on Friday, July 6, to 9:00 on Saturday, July 7, 2018 for analysis. For comparison, we use the data of the same time periods from June 8 (Friday) to June 9 (Saturday), 2018, one month prior to the event. Data with a detection time interval over 30 minutes were excluded from analysis. The number of unique IDs is 3,009. The population of Mabi town is about 23,000. As a feature of these data, only the location data of smartphones that launch the applications is collected; therefore, the results do not contain the total number data, and there is some bias.

[1]Blogwatcher: https://www.blogwatcher.co.jp/

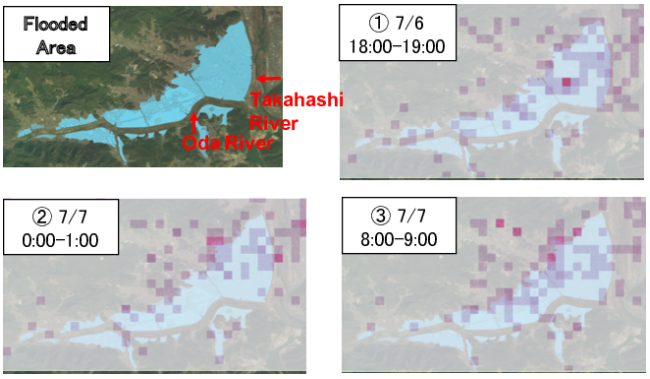

Fig. 3. Flooded Area and Population Distribution from Location Data

C. Population Distribution in the Flooded Area

Figure 3 shows the population distribution of Mabi town. Calculation of population distribution is not included in the procedure of this method. We tried visualizing the population distribution in order to confirm whether it is possible to detect an anomaly area with simple analysis. The flooded area is on both sides of the Oda River and the west side of the Takahashi River. In Figure 3, we present the flooded area divided into 250 meter grids and the population distribution at ① 18:00-19:00, ② 0:00-1:00, and ③ 8:00-9:00. Figure 3: ① 18:00-19:00 is before the occurrence of flooding in this area. There are many distributions on the north side of the river.

Figure 3: ② 0:00-1:00 shows the population distribution when flooding occurred in the Oda River. The flooding of the Oda River occurred at 0:30. Comparing with Figure 3: ① 18:00-19:00 and ② 0:00-1:00, the distribution is moving slightly from the periphery of the river. Figure 3: ③ 8:00-9:00 shows the population distribution after flood occurrence. Comparing these three time periods, the distribution gradually changed for each period; nevertheless, we found that there were no large changes in those trends.

D. People Movement Trends in a Flood Situation

With respect to the whole area of Mabi town, we estimated the moving speed from the difference of the location data. Then, we classified the moving speeds into three groups. Figure 4(a) and Figure 4(b) show the ratio of the three groups with a bar chart. Each moving speed corresponds to the following: blue in a stationary state, orange during walking, and green in a moving vehicle. For each moving speed, a blue bar corresponds to a stationary state, an orange bar corresponds to walking, and a green bar corresponds to a moving by vehicle. Additionally, the green and orange bars indicate the ratio of people moving.

In the regular time of Figure 4(a), after 18:00, the ratio of people moving decreases. By contrast, in the flooding situation of Figure 4(b), we found that there are many people moving even after 22:00. Furthermore, the black line chart shows the number of people estimated to be moving. In the regular time of Figure 4(a), the number of people moving decreases until 4:00. From 5:00, the number of moving people increases. In

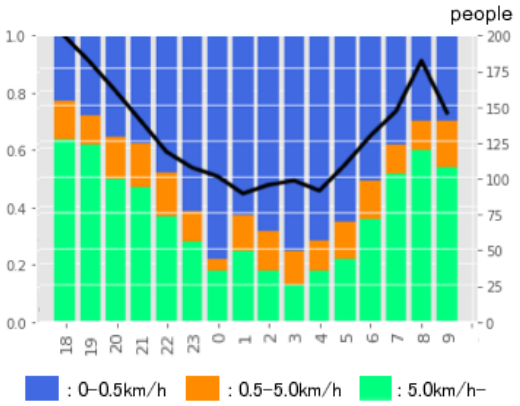

(a) Regular Time

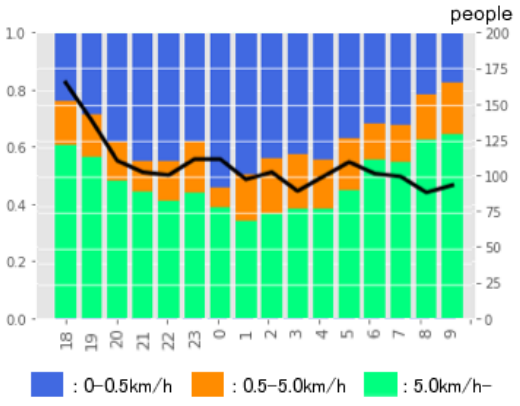

(b) Flooding Situation

Fig. 4. Ratio of Location Data Number by Moving Speed

contrast, the trend in the flooding situation was totally different from that of regular times.

The number of moving people is increasing at 22:00 (when the evacuation advisory was issued), at 0:00 (when the evacuation order was issued), and at 1:00 (after the evacuation order was issued). We found that there was a different moving trend from the regular time, and the number of people moving increased during the evacuation advisory and evacuation orders.

E. Result of Estimation Method

The result of clustering is shown in Figure 5. We perform the clustering process by the k-medoids method, after deleting the grid with extremely low number of location data (1 or fewer IDs in 15 minutes) using the data from 0:00 June 8 to 23:59 June 9 one month before the flooding. 26 grids have remained. Figure 5 shows the result of clustering with 5 clusters for the car speed data. As a result of clustering, there are both grids with large DTW distance values and small values. Since there were many grids with few affected people, this method classified as different cluster even for grid which does not differ much like cluster 0 and cluster 2. However, it is difficult to determine the tendency of grid with few affected people, hence, it is necessary to consider the

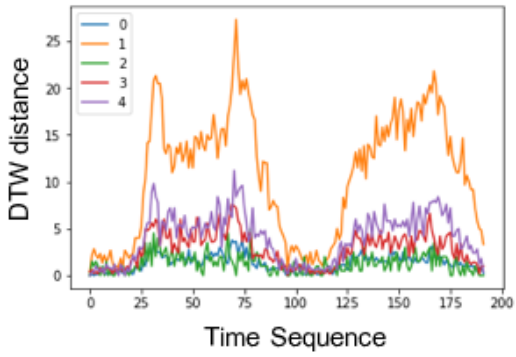

Fig. 5. Clustering Result (Regular Time)

number of affected people that can be detected and to develop a method to dynamically calculate the optimum number of clusters. From 0:00 to 23:59 June 8 ($t = 0 - 96$), peaks were observed in the morning and evening in all clusters. These peaks are considered to be commuter movement. Since June 9 ($t = 97 - 182$) was Saturday, no peak was observed.

Using wDTW, we processed the regular time clustering result and the data from 0:00 June 6 to 23:59 June 7 when flooding occurred. Figure 6 shows the result of wDTW. Figure 6(a) is the result of wDTW at 22:00 when the evacuation recommendation was issued throughout the city. From the results of interviews with neighboring residents, it is known that flooding occurred in various places of the city around this time. The light blue part shows the area that is finally flooded. This area almost coincides with the area detected by wDTW. Figure 6(b) is representative of the time when the evacuation order was issued to the south of the Oda River. A local agency issued an evacuation order to the north side of the Oda River at the time as shown in Figure 6(c). Even at this time, the area actually inundated was consistent with the result of the anomaly estimation.

Using the Gini coefficient, we calculated inequality metrics. At 22:00, as shown in Figure 6(a), the value of Gini coefficient increased in 11 grids. Among these grids, the 7 inundated grids were observed. The remaining 4 grids had no inundation. Overall, 2 grids showed areas where an explosion and a fire occurred due to inundation around 23:30. There is a possibility that an anomaly event had occurred around this time. The maximum value of the spatial Gini coefficient at this time was 6.81, and the Gini coefficient was 3.30.

F. Discussion Regarding Estimation of the Road Condition

We describe the purpose of analysis for grids detected as anomaly areas using the spatial Gini coefficient. This approach is expected to judge passability, that is, whether or not a road inside the grid can be passed, based on the tracking results of the route for the area where the spatial Gini coefficient shows high inequality. We mapped the route of people who moved for each time period to estimate the routes that each piece of personal location data moved (Figure 7). For ②, until 24:00 July 6, there is movement even in the flooded area. We can see

(a) 22:00, July 6 (b) 23:45, July 6 (c) 01:30, July 7

Fig. 6. wDTW Results

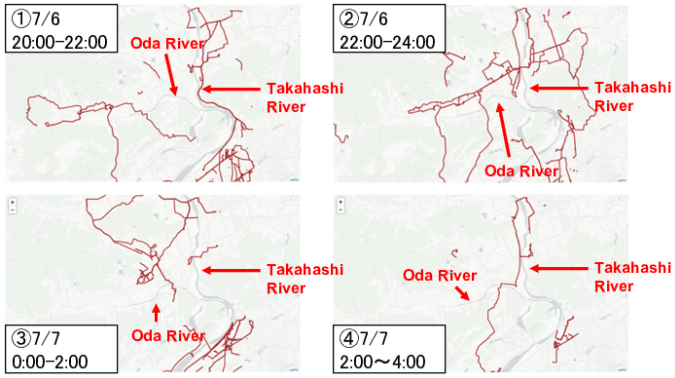

Fig. 7. Traffic Results of the Flooded Area

that the moving IDs are decreasing as time passes. In ① and ②, some IDs pass the west side of the Oda River, despite no movement being observed in ③. Namely, there is a possibility that the road on the west side was not passable. Using these data, we believe that it is possible to estimate passability of a specific road. We expect that this passability estimation can be used for an evacuation route recommendation system.

V. Conclusion

This paper proposed a flood estimation method without river monitoring data using personal location data. Many people died due to evacuation delay since they could not know a flood occurred in the area where observation equipment was not installed. This research estimated flood areas using GPS data collected from the smartphone owned by the affected people. This anomaly detection method calculated the characteristics of location data; moreover, the method investigated the spatial and temporal changes of the characteristics. We classified the location data of each 2-km grid with clustering using the k-medoids method. Then, we compared the characteristics of clustered data to location data at the time when there was a danger of flood occurrence. We improved the DTW method as the windowed DTW method, which was used for quantifying the similarity between several time series data. Then, for detection of the anomaly area, we compared the characteristics of each grid using inequality metrics.

Our method showed that the area actually inundated was consistent with the flood estimation result. At the same time, there were some areas that were estimated as anomaly areas, despite the lack of flooding. It is necessary to improve this method to accurately estimate flooding areas using data such as precipitation amount or flood vulnerability. Although this paper is based on a small data in flood situation, it is necessary to evaluate whether this method can be applied even flood damage in other areas. Since this area was a region with less population, it was detected every 2-km grid. In case of an area where more personal location data can be collected, there is a possibility of detecting flood area with more detailed spatial resolution. We are planning to detect anomaly area and to evaluate the accuracy by using personal location data of various flood disasters. We classified moving speed based on distance and time. This paper used only the data collected at intervals of less than 30 minutes. In order to use big data as personal location data, it is desirable to use data with a large time interval. We will prepare learning data to improve detection accuracy by machine learning method.

In addition, we considered a method of estimating the road condition of the anomaly area. In this paper, we showed a method to estimate flooded area using personal location data. It is necessary for a system which support to evacuate the affected people remaining in the estimated flooded area. In areas where flood damage occurred, we found that the number of moving IDs decreased as the flood damage area expanded, mapping the route of people who moved for each time period. Using these data, we estimated the passability of a specific road in an anomaly area for an evacuation route recommendation system.

Acknowledgment

This research was supported by the MIC/SCOPE #172106102.

References

[1] Intergovernmental Panel on Climate Change Fifth Assessment Report (AR5), Retrieved April 17, 2018, from https://www.ipcc.ch/report/ar5/, 2018.

[2] Milly, P. Christopher D., Wetherald, Richard T., Dunne, K. A., Delworth, Thomas L, Increasing Risk of Great Floods in a Changing Climate, Nature, Nature Publishing Group, Vol.415, No.6871, page514, 2002.

[3] Hirabayashi, Y., Mahendran, R., Koirala, S., and Konoshima, L., Yamazaki, D., Watanabe, S., Kim, H., and Kanae, S., Global Flood Risk under Climate Change, Nature Climate Change, Nature Publishing Group, Vol.3, No.9, page816, 2013.

[4] Plate, Erich J., Flood Risk and Flood Management, Journal of Hydrology, Elsevier, Vol.267, No.1-2, pp.2–11, 2002.
[5] Sayers, P. B., Hall, J. W., Meadowcroft, I. C., Towards Risk-based Flood Hazard Management in the UK, In Proceedings of the Institution of Civil Engineers-Civil Engineering, Thomas Telford Ltd, Vol.150, No.5, pp.36–42, 2002.
[6] Prudhomme, C., Wilby, R.L., Crooks, S., Kay, A. L., Reynard, N. S., Scenario-neutral Approach to Climate Change Impact Studies: Application to Flood Risk, Journal of Hydrology, Elsevier, Vol.390, No.3-4, pp.198–209, 2010.
[7] Islam, M. A., Islam, T., Syrus, M. A., Ahmed, N., Implementation of Flash Flood Monitoring System based on Wireless Sensor Network in Bangladesh, In Proceeding of the IEEE 2014 International Conference on Informatics, Electronics & Vision (ICIEV), pp.1-6, 2014.
[8] Mousa, M., Oudat, E., Claudel, C., A Novel Dual Traffic/Flash Flood Monitoring System Using Passive Infrared/Ultrasonic Sensors, In Proceeding of the IEEE 12th International Conference on Mobile Ad Hoc and Sensor Systems (MASS), pp.388-397, 2015.
[9] Khan, F., Memon, S., Jokhio, I. A., Jokhio, S. H., Wireless Sensor Network based Flood/Drought Forecasting System, In Proceeding of the IEEE Sensors 2015, pp.1-4, 2015.
[10] Anthone, A., Mynor, V., Oishi, S., A Wireless Mesh Sensor Network Framework For River Flood Detection And Emergency Communications In Case Of Disaster, CUNY Academic Works. http://academicworks.cuny.edu/cc_conf_hic/90, 2014.
[11] Elshorbagy, A., Corzo, G., Srinivasulu, S., Solomatine, D., Experimental Investigation of the Predictive Capabilities of Data Driven Modeling Techniques in Hydrology—part 2: Application, Hydrology and Earth System Sciences, vol.14, pp.1943-1961, 2010.
[12] Rafieeinasab, A., Norouzi, A., Kim, S., Habibi, H., Nazari, B., Seo, D., Lee, H., Cosgrove, B., Cui, Z., Toward High-resolution Flash Flood Prediction in Large Urban Areas − Analysis of Sensitivity to Spatiotemporal Resolution of Rainfall Input and Hydrologic Modeling, Journal of Hydrology, vol.531, part 2, pp.370-388, 2015.
[13] Ruslan, F. A., Samad, A. M., Zain, Z. M., Adnan, R., Flood Prediction using NARX Neural Network and EKF Prediction Technique: A Comparative Study, In Proceeding of the IEEE 3rd International Conference on System Engineering and Technology (ICSET), pp.203-208, 2013.
[14] Sakaki, T., Okazaki, M., Matsuo, Y., Earthquake Shakes Twitter Users: Real-time Event Detection by Social Sensors, In Proceedings of the 19th International Conference on World Wide Web, pp.851-860, ACM, 2010.
[15] Jianshu, W., Lee, B., Event Detection in Twitter, In Proceedings of the Fifth International AAAI Conference on Weblogs and Social Media (ICWSM11), pp.401-408, 2011.
[16] Seonhwa, C., Bae, B., The Real-time Monitoring System of Social Big Data for Disaster Management, Computer science and its applications, Springer, pp.809-815, 2015.
[17] Witayangkurn, A., Horanont, T., Sekimoto, Y., Shibasaki, R., Anomalous Event Detection on Large-scale GPS Data from Mobile Phones using Hidden Markov Model and Cloud Platform, In Proceedings of the 2013 ACM conference on Pervasive and ubiquitous computing adjunct publication (UbiComp'13), ACM, pp.1219-1228, 2013.
[18] Madey, G. R., Barabasi, A., Chawla, N. V., C., Gonzalez, M., Hachen, D., Lantz, B., Pawling, A., Schoenharl, T., Szabo, G., Wang, P., Yan, P., Enhanced Situational Awareness: Application of DDDAS Concepts to Emergency and Disaster Management, In Proceedings of the International Conference on Computational Science, pp.1090-1097, Springer, 2007.
[19] Gerla, M., Lee, E., Pau, G., Lee, U., Internet of vehicles: From intelligent grid to autonomous cars and vehicular clouds, In Proceedings of 2014 IEEE World Forum on the Internet of Things (WF-IoT), IEEE, pp.241-246, 2014.
[20] Yamagata Y., Murakami D., Wu Y., Yang P., Yoshida T., Binder R., In Proceedings of the 10th International Conference on Applied Energy (ICAE), Elsevier, 6 pages, 2018.